



**Weierstrass Institute for
Applied Analysis and Stochastics**

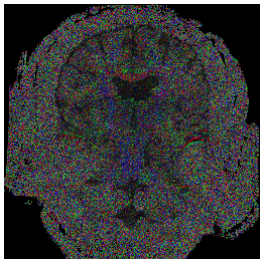
Modeling high resolution MRI: Statistical issues

Jörg Polzehl (joint work with Karsten Tabelow)

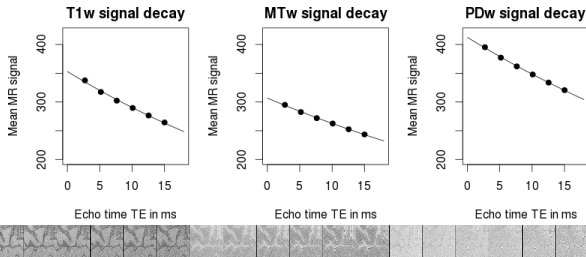
- Motivation
- The distribution of MRI data (is it really Rician)
- Effects of preprocessing
- What is the relevant SNR of the data
- Smoothing MRI data
- Something to learn in the HCP high resolution dMRI experiment
- Conclusions

Driving issue: Interest in very detailed structure:

- White matter - Cortex boundary (Kurtosis imaging, $500\mu m$)
- Fiber crossings and bifurcations (DWI, $800\mu m$, high b-values)
- Multiparameter mapping (Layer structure in cortex $300\mu m$, in-vivo diagnostics)



Data: Siawoosh
Mohammadi



Data: Nick Weiskopf



Figure: Kasuga Huang (Wikimedia)

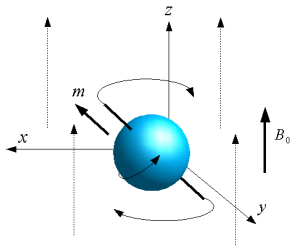


Figure: Franz Wilhelmstötter (Wikimedia)

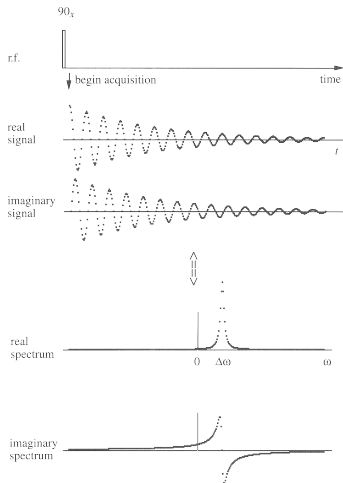


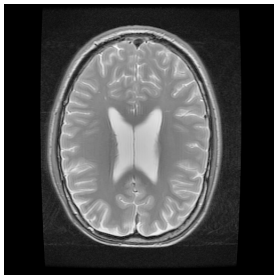
Fig. 2.7 Free Induction Decay (FID) following a single 90° r.f. pulse. The real and imaginary parts of the signal correspond to the in-phase and quadrature receiver outputs. The signal is depicted with receiver phase $\phi = 0$ and, on complex Fourier transformation, gives real absorption and imaginary dispersion spectra at the offset frequency, $\Delta\omega = \omega_0 - \omega$.

From O. Friman "Adaptive Analysis of Functional MRI Data", PhD Thesis, 2003

- Measurements in **K-Space**: Complex signal (amplitude and phase) at readout time carries thermal (Gaussian) noise
- complex image generated by **Fast Fourier Transform (FFT)**
- **magnitude images** as modulus of the complex image



T_1 -weighted



T_2 -weighted

thanks to: F. Godtliebsen
(University Tromsø), H.U. Voss
(Weill Cornell Medical College,
NY) and

- complex signal in K-space (one coil):

$$s_c(k) \sim N(x_c(k), \sigma_K^2)$$

- FFT provides complex valued image

$$S_c(x) \sim N(\xi_c(x), \sigma_I^2)$$

- MR image: $S(x)$ usually obtained as magnitude image

$$\text{Notation: } S_i = |S(x_i)|$$

- Signal distribution: Rician distribution

$$S_i/\sigma_I \sim \chi_{2, \eta_i} \text{ with } \eta_i = |\xi_c(x_i)|/\sigma_I$$

- Problem:

$$\mathbf{E}S_i/\sigma_I > \eta_i$$

gap severe if $\eta \ll 4$



Image: F. Godtliobsen (Tromsø)

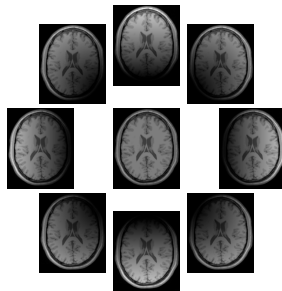
Increase of **sensitivity** and reduction of **time** by

Methods:

- multiple Receiver Coils
- sensitivity encoding
- reduced field of view
- subsampling in K-space
- simultaneous slice aquisitions
- partial parallel aquisitions
- ...

Consequences:

- need for sophisticated image reconstruction
- determines signal distribution
- induces spatial correlations (see talk by D. Rowe at Opening WS)



8-coil system (noiseless situation):
Images from receiver coils and
combined image

- 8 – 32 spherically arranged receiver coils
- inhomogeneous coil sensitivities, correlation between receiver coils
- image reconstruction from coils $k = 1, \dots, K$ as SENSE-1: (Sotiropoulos 2013, Pruessmann 1999)

$$S_i = \left| \sum c_{ik} S_k(x_i) \right|$$

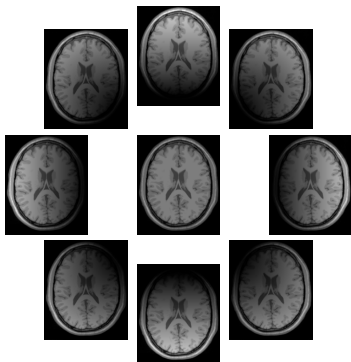
efficient, known distribution, location dependent $\sigma_{I,i}$, Rician distribution

$$S_i / \sigma_{I,i} \sim \chi_{2, \eta_i}$$

$$\eta_i = \left| \sum c_{ik} \xi_k(x_i) \right| / \sigma_{I,i}$$

$\sigma_{I,i}$ depends on coil sensitivities, correlations

→ Rician after image reconstruction



8-coil system (noiseless situation):
Images from receiver coils and
combined image

Preprocessing steps:

- susceptibility correction (DWI)
- Eddy current correction (DWI)
- Image registration
- ...

Effects:

- All preprocessing steps involve spatial interpolation
- Change data distribution to a linear combination of Ricians
- Designed to keep expected value
- Decrease the variance
- Resulting distribution is closer to a Gaussian
- **Problem:**

$$ES_i/\sigma_I > \eta_i$$

is preserved !!

- σ_I refers to the unprocessed data

- Problem: $\mathbf{E}S_i/\sigma_I > \eta_i$ is preserved !!
- σ_I refers to the unprocessed data

To address this we need to analyze unprocessed Data !!!

Properties of scale σ_I

- depends on parameters of the image reconstruction algorithm (scanner geometry, scanner protocols)
- parameters are usually unknown
- spatially varying (larger in the center)

Need to estimate σ_I :

K. Tabelow, H.U. Voss, J. Polzehl (2015).

Local estimation of the noise level in MRI using structural adaptation

Medical Image Analysis, DOI: [10.1016j.media.2014.10.008](https://doi.org/10.1016/j.media.2014.10.008).

Assumptions:

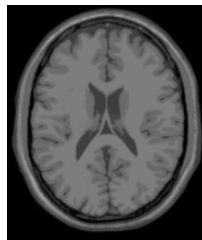
- $S_i/\sigma_i \sim \chi_{2L, \zeta_i/\sigma_i}$
- ζ_i local constant
- local homogeneity of tissue and fiber direction (diffusivity)
- σ_i slowly varying in space
- smooth variation of coil sensitivities

Sequential multi-scale algorithm

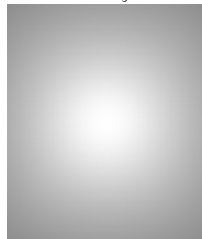
- Using local weighted likelihood estimates for ζ_i and σ_i
- Robust (median) smoothing for estimated σ_i
- Weighting schemes by localization in image space and adaptation in parameter space

Alternatives

- Global estimates from **background**
- Methods from Aja-Fernandez (201x), Landman (2009)



local variation of ζ_0



local variation of σ for artificial 8-coil system and SENSE-1

Adaptive smoothing of dMRI data:

- Needs to take image structure into account (adaptation)
- Single images do not have enough information for successful adaptation
- Model based adaptation depends on adequate modeling
- \rightarrow Smoothing in $R^3 \times S^2$
- Adaptation based on data distribution and correct assessment of data variability
- smooth unprocessed or preprocessed data ???

S. Becker, K. Tabelow, S. Mohammadi, N. Weiskopf, J. Polzehl (2014).

Adaptive smoothing of multi-shell diffusion-weighted magnetic resonance data by msPOAS.
Neuroimage, 95, pp. 90–105.

Diffusion Tensor Model: (Homogeneity within a voxel, no effect of fiber structure)

$$P(\vec{R}, \tau) = P(r\vec{g}, \tau) = \frac{1}{\sqrt{\det \mathcal{D}(4\pi\tau)^3}} \exp\left(-r^2 \frac{\vec{g}^T \mathcal{D}^{-1} \vec{g}}{4\tau}\right).$$

- Theoretical signal:**

$$\zeta_{b,g}(\theta_i) = \zeta_{0,i} e^{-bg^T \mathcal{D}_i g}$$

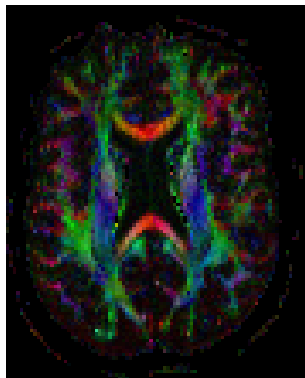
- Fully characterized by the Diffusion Tensor \mathcal{D}**

- Mean diffusivity**

$$Tr(\mathcal{D}) = \lambda_1 + \lambda_2 + \lambda_3 = 3\bar{\lambda}$$

- Fractional anisotropy (FA)**

$$FA = \left(\frac{3}{2} \frac{(\lambda_1 - \bar{\lambda})^2 + (\lambda_2 - \bar{\lambda})^2 + (\lambda_3 - \bar{\lambda})^2}{\lambda_1^2 + \lambda_2^2 + \lambda_3^2} \right)^{1/2}$$



Visualization: Color coded FA maps

- Theoretical noise-free signal : $\zeta_{b,g}(\theta)$
- Expected signal

$$\mathbf{E}S_{b,g} = \mu(\zeta_{b,g}(\theta), \sigma_{b,g}) = \sigma_{b,g} \sqrt{\frac{\pi}{2}} \mathbf{L}_{1/2}^{(L-1)} \left(-\frac{\zeta_{b,g}^2(\theta)}{2\sigma_{b,g}^2} \right).$$

$$\mathbf{L}_{1/2}^{(L-1)}(x) = \frac{\Gamma(L+1/2)}{\Gamma(3/2)\Gamma(L)} \mathbf{M}(-1/2, L, x)$$

\mathbf{L} - generalized Laguerre polynomial, \mathbf{M} - confluent hypergeometric function.

- variance of the preprocessed signal:

$$v_{bg} = C_{bg} [2L\sigma_{b,g}^2 + \zeta_{b,g}(\theta)^2 - \mu^2(\zeta_{b,g}(\theta), \sigma_{b,g})]$$

where $C_{bg} \leq 1$ - variance reduction due to preprocessing.

- Absolute discrepancy for Rician data ($L = 1$)

ζ/σ	0.0	1.0	2.0	3.0	4.0	6.0	8.0
$(\mu(\zeta, \sigma) - \zeta)/\sigma$	1.25	0.55	0.27	0.17	0.13	0.084	0.063

■ **Nonlinear regression:**

$$S_{b,g} = \zeta_{b,g}(\theta') + \epsilon_{b,g}, \quad \mathbf{E} \epsilon_{b,g} = 0 \quad \mathbf{Var} \epsilon_{b,g} < \infty$$

$$\hat{\theta} = (\hat{\zeta}_0, \vec{\hat{D}}) = \operatorname{argmin}_{\theta'} \sum_{b,g} w_{b,g} \left[S_{b,g} - \zeta_{b,g}(\theta') \right]^2$$

Estimates parameters in a weighted inadequate least squares approximation (WILSA).

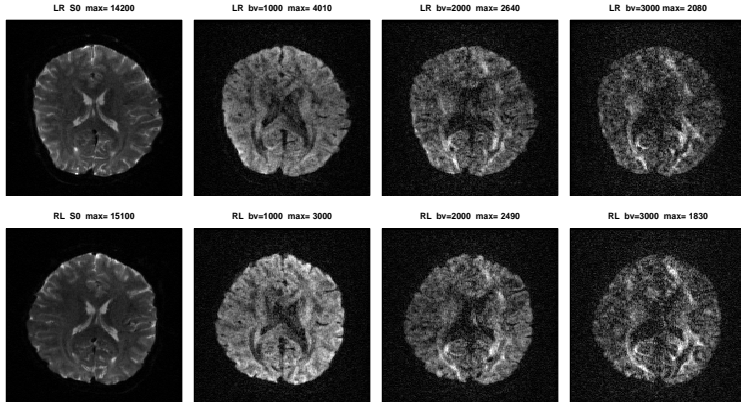
Projection parameters:

$$\bar{\theta} = \operatorname{argmin}_{\theta'} \sum_{b,g} w_{b,g} \left[\mu(\zeta_{b,g}(\theta'), \sigma_{b,g}) - \zeta_{b,g}(\theta') \right]^2$$

■ **Quasi-Likelihood:** with $w_{b,g} = 1/v_{b,g}$

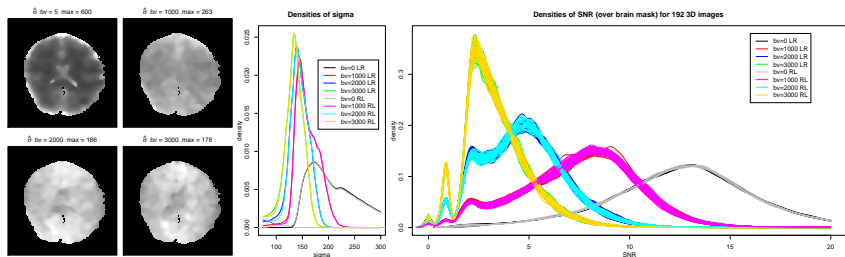
$$\tilde{\theta} = \operatorname{argmin}_{\theta'} \sum_{b,g} w_{b,g} \left[S_{b,g} - \mu(\zeta_{b,g}(\theta'), \sigma_{b,g}) \right]^2$$

Estimates parameters in adequate model by weighted least squares WLSE



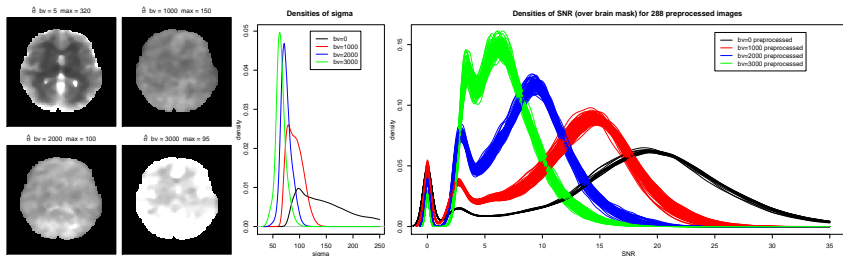
Unprocessed HCP data for LR / RL phase encoding, b-values 0, 1000, 2000, 3000. Signal attenuation at larger b-values leads to deteriorating SNR

[*] Data were provided by the Human Connectome Project, WU-Minn Consortium (Principal Investigators: David Van Essen and Kamil Ugurbil; 1U54MH091657) funded by the 16 NIH Institutes and Centers that support the NIH Blueprint for Neuroscience Research; and by the McDonnell Center for Systems Neuroscience at Washington University



- Left: Estimated local scale parameter σ for approximate b-values 5 s/mm^2 (S_0), 1000 s/mm^2 , 2000 s/mm^2 and 3000 s/mm^2
- Center: Densities of estimated σ (2 out of 6 runs, a total of 192 image volumes, 96 with right-to-left (RL) and 96 with left-to-right (LR) phase encoding directions)
- Right: Densities of estimated SNR ζ/σ for same volumes.
- percentage of voxel (in brain mask) with $SNR < 4$

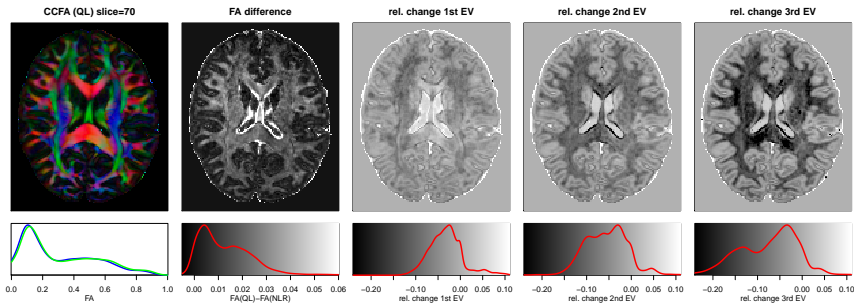
b-value in s/mm^2	0	1000	2000	3000
run with LR phase encoding	4%	14%	38%	71%
run with RL phase encoding	3%	13%	37%	71%



- Left: Estimated local scale parameter σ for approximate b-values 5 s/mm² (S_0), 1000 s/mm², 2000 s/mm² and 3000 s/mm²
- Center: Densities of estimated σ (288 image volumes)
- Right: Densities of estimated SNR ζ/σ for same volumes.
- percentage of voxel (in brain mask) with $SNR < 4$ significantly reduced (mainly regions with CSF)
- Variance reduced by a factor of 4
- Bias problem hidden

- Corrected for susceptibility, Eddy currents, ..., registered to common space.
- leads to variance reduction and spatial correlation, but leaves mean signal unchanged.

Comparison of DTI results:



QL with median b-value dependent σ (obtained from unprocessed data)(green) and NLR (blue).
 NLR shows a tissue specific negative bias in FA and positive bias in all tensor eigenvalues.

- Use of MR in in-vivo histology demands for **increased spatial resolution**
- Assessing Bias provides comparability between subjects, dates, scanning devices
- Image **SNR** proportional to **voxel volume**
- Advanced dMRI modeling needs multiple **(high) b-values**
- Image **SNR** may decay **exponentially in b-values**
- **Severe bias** of (inadequate) NLR estimates in case of low SNR
- Adequate modeling requires information about **signal distribution** (prefer SENSE over GRAPPA)
- Need to calculate or estimate **noise level of unprocessed data**
- Modeling of processed data by **Quasi-Likelihood** using estimated noise level
- Signal distribution and estimated noise level also needed for **adaptive smoothing (msPOAS)**

-  ■ Karsten Tabelow (WIAS)
-  ■ Henning U. Voss (Weill Medical College, Cornell Univ., New York)
-  ■ Nikolaus Weiskopf (Wellcome Trust Centre for Neuroimaging, UCL London)
-  ■ Siawoosh Mohammadi (UCL London and Univ. of Hamburg)
-  ■ Michael Deppe (Morphometrie und funktionelle Bildgebung, Univ.Kl. Münster)
-  ■ Alfred Anwander (MPI for Human Cognitive and Brain Sciences Leipzig)
-  ■ Robin M. Heidemann (Magnetic Resonance Division, Siemens)
-  ■ Remco Duits (BioMedical Image Analysis, Univ. of Eindhoven)

References:



J. Polzehl, K. Tabelow (2015).

Modeling high resolution MRI: Statistical issues with low SNR
WIAS- preprint 2179.



K. Tabelow, H.U. Voss, J. Polzehl (2015).

Local estimation of the noise level in MRI using structural adaptation
Medical Image Analysis, DOI: 10.1016/j.media.2014.10.008.



S. Mohammadi, K. Tabelow, L. Ruthotto, T. Feiweier, J. Polzehl, N. Weiskopf (2015).

High-resolution diffusion kurtosis imaging at 3T enabled by advanced post-processing
Frontiers in Neuroscience, 122014, 8 (427):1-14.



S. Becker, K. Tabelow, S. Mohammadi, N. Weiskopf, J. Polzehl (2014).

Adaptive smoothing of multi-shell diffusion-weighted magnetic resonance data by msPOAS.
Neuroimage, 95, pp. 90–105.



J. Polzehl, V. Spokoiny (2006).

Propagation-separation approach for local likelihood estimation,
Probability Theory and Related Fields, 135: 335–362.

Software:

- R-package dti, <https://cran.r-project.org/>
- ACID toolbox, <http://www.diffusio.tools.com/>